

Polyelectrolyte Multilayering on a Charged Sphere

René Messina,^{*} Christian Holm,[†] and Kurt Kremer[‡]

*Max-Planck-Institut für Polymerforschung,
Ackermannweg 10, 55128 Mainz, Germany*

(Dated: August 28, 2018)

Abstract

The adsorption of highly *oppositely* charged flexible polyelectrolytes on a charged sphere is investigated by means of Monte Carlo simulations in a fashion which resembles the layer-by-layer deposition technique introduced by Decher. Electroneutrality is insured at each step by the presence of monovalent counterions (anions and cations). We study in detail the structure of the *equilibrium* complex. Our investigations of the first few layer formations strongly suggest that multilayering on a charged colloidal sphere is not possible as an equilibrium process with purely electrostatic interactions. We especially focus on the influence of specific (non-electrostatic) short range attractive interactions (e.g., Van der Waals) on the stability of the multilayers.

arXiv:cond-mat/0212291v2 [cond-mat.soft] 16 Jun 2003

^{*}Electronic address: messina@thphy.uni-duesseldorf.de; Permanent address: Institut für theoretische Physik

II, Heinrich-Heine-Universität Düsseldorf, Universitätsstrasse 1, D-40225 Düsseldorf, Germany

[†]Electronic address: holm@mpip-mainz.mpg.de

[‡]Electronic address: kremer@mpip-mainz.mpg.de

I. INTRODUCTION

Polyelectrolyte multilayer thin films are made of alternating layers of polycations (PCs) and polyanions (PAs). The so-called layer by layer method, first introduced in *planar* geometry by Decher, consists in a successive adsorption of the polyions onto a charged surface and has proved to be extremely efficient [1, 2]. Due to the many potential technological applications such as biosensing [3], catalysis [4], optical devices [5] etc., this process is nowadays widely used. Various techniques are employed to control the polymer multilayer buildup such as optical [6, 7] and neutron [8, 9] reflectometry, AFM [10], UV spectroscopy [11], NMR techniques [12], and others. Some experiments (see e.g., Ref. [13]) were devoted to the basic mechanisms governing polyelectrolyte multilayering on planar mica-surfaces where especially, the role of surface charge overcompensation was pointed out.

Another very interesting application is provided by the polyelectrolyte coating of *spherical* metallic nanoparticles [14, 15]. This process can modify in a well controlled way the physico-chemical surface properties of the colloidal particle. Despite of the huge amount of experimental works, the detailed understanding of the multilayering process is still rather unclear, especially for a charged colloidal sphere. Hence the study of polyelectrolyte multilayering is motivated by both experimental and theoretical interests.

On the theoretical side, the literature on this subject is rather poor. Based on Debye-Hückel approximations for the electrostatic interactions and including lateral correlations by considering different typical semiflexible polyelectrolyte-layer structures, Netz and Joanny [16] found a remarkable stability of the periodic structure of the multilayers in planar geometry. For weakly charged flexible polyelectrolytes at high ionic strength qualitative agreements between theory [17], based on scaling laws, and experimental observations [9, 18] have been provided. The driving force of all these multilayering processes is of electrostatic origin and it is based on an overcharging mechanism, where the first layer overcharges the macroion and the subsequent layers overcharge the layers underneath. However, the role of non-electrostatic interactions though pointed out in Ref. [17, 19] is not clear. In particular, it is still open whether the layer build up is an equilibrium- or out of equilibrium process, which resembles more a succession of dynamically trapped states. Therefore we do not know whether or not the complex polyelectrolyte is in *thermodynamical equilibrium*. This point has also been emphasized in a recent experimental work on planar multilayers

[7] where considerable kinetic effects were reported. So far, there are nor analytical results neither simulation data for multilayering formation onto charged spheres.

The goal of this paper is to study the underlying physics involved in the polyelectrolyte multilayering onto a charged colloidal sphere by means of MC simulations. The paper is organized as follows: Sec. II is devoted to the description of our MC simulation method. The relevant target quantities are specified in Sec. III. The single chain adsorption is studied in Sec. IV, and the polyelectrolyte bilayering in Sec. V. Then the multilayering process is investigated in Sec. VI. The case of short polyelectrolyte chains is considered in Sec. VII. Finally, Sec. VIII contains some brief concluding remarks.

II. SIMULATION METHOD

The setup of the system under consideration is very similar to those recently investigated by means of molecular dynamics simulations [20, 21]. Within the framework of the primitive model we consider one charged colloidal sphere characterized by a radius a ($= 4.5\sigma$) and a bare charge $Q_M = -Z_M e$ (where e is the elementary charge and $Z_M = 40$) surrounded by Z_M neutralizing monovalent ($Z_c = 1$) counterions and an implicit solvent (water) of relative dielectric permittivity $\epsilon_r \approx 80$. In the remaining of the paper, we will refer to the term *macroion* as the charged colloidal sphere. Polyelectrolyte chains (N_+ PCs and N_- PAs) are made up of N_m *monovalent* monomers ($Z_m = 1$) of diameter σ . For the sake of simplicity, we only consider here symmetrical complexes where PC and PA chains have the same length and carry the same charge in absolute value. To each charged PC or PA we also add N_m small *monovalent* ($Z_c = 1$) counterions (anions and cations countering the charge of the polyelectrolytes) of diameter σ , hence always a charge neutral entity was added. Thereby all the microions have the same valence $Z = Z_c = Z_m = 1$ as well as the same diameter σ . Added salt of course would even weaken the effects observed and would be especially important for the case of an adsorption interaction between macroion and polyelectrolyte.

All these particles making up the system are confined in an impermeable spherical cell of radius $R = 60\sigma$. The spherical macroion is held fixed and located at the center of the cell. To avoid the appearance of image charges [22], we assume that the macroion has the same dielectric constant as the solvent.

Standard canonical MC simulations following the Metropolis scheme were used [23, 24].

The total energy of interaction of the system can be written as

$$U_{tot} = \sum_{i,i<j} U_{hs} + U_{coul} + U_{FENE} + U_{LJ} + U_{vdw}, \quad (1)$$

where all the contributions of the pair potentials in Eq. (1) are described in detail below.

Excluded volume interactions are modeled via a hard sphere potential U_{hs} [25] defined as follows

$$U_{hs}(r) = \begin{cases} \infty, & \text{for } r < r_{cut} \\ 0, & \text{for } r \geq r_{cut} \end{cases} \quad (2)$$

where $r_{cut} = \sigma$ for the microion-microion excluded volume interaction, and $r_{cut} = a + \sigma/2$ for the macroion-microion excluded volume interaction. Hence the center-center distance of closest approach between the macroion and a microion is $r_0 = a + \sigma/2 = 5\sigma$.

The pair electrostatic interaction between two ions i and j (where i and j can be either a microion or the macroion) reads

$$U_{coul}(r_{ij}) = \pm k_B T l_B \frac{Z_i Z_j}{r_{ij}}, \quad (3)$$

where $+(-)$ applies to charges of the same (opposite) sign and $l_B = e^2/4\pi\epsilon_0\epsilon_r k_B T$ is the Bjerrum length corresponding to the distance at which two elementary charges interact with $k_B T$. To link our simulation parameters to experimental units and room temperature ($T = 298\text{K}$) we choose $\sigma = 4.25 \text{ \AA}$ leading to the Bjerrum length of water $l_B = 1.68\sigma = 7.14 \text{ \AA}$ and to a macroion surface charge density of $0.14 \cdot \text{Cm}^{-2}$.

The polyelectrolyte chain connectivity is modeled by using a standard FENE potential in good solvent (see, e.g., [26]), which reads

$$U_{FENE}(r) = \begin{cases} -\frac{1}{2}\kappa R_0^2 \ln \left[1 - \frac{r^2}{R_0^2} \right], & \text{for } r < R_0 \\ \infty, & \text{for } r \geq R_0 \end{cases} \quad (4)$$

where we chose $\kappa = 27k_B T/\sigma^2$ and $R_0 = 1.5\sigma$. The excluded volume interaction between chain monomers is taken into account via a purely repulsive Lennard-Jones (LJ) potential

given by

$$U_{LJ}(r) = \begin{cases} 4\epsilon \left[\left(\frac{\sigma}{r}\right)^{12} - \left(\frac{\sigma}{r}\right)^6 \right] + \epsilon, & \text{for } r \leq 2^{1/6}\sigma \\ 0, & \text{for } r > 2^{1/6}\sigma \end{cases} \quad (5)$$

where $\epsilon = k_B T$. These parameters lead to an equilibrium bond length $l = 0.98\sigma$.

An important interaction in the multilayering process addressed in this study is the *non-electrostatic short ranged attraction*, U_{vdw} , between the macroion and the PC chain. To account for this kind of interaction, we choose without loss of generality a van der Waals (VDW) potential of interaction between the macroion and a PC monomer that is given by

$$U_{vdw}(r) = -\epsilon\chi_{vdw} \left(\frac{\sigma}{r - r_0 + \sigma} \right)^6 \quad \text{for } r \geq r_0, \quad (6)$$

where χ_{vdw} is a positive dimensionless parameter describing the strength of the attraction. Thereby, at contact (i.e., $r = r_0$), the magnitude of the attraction is $\chi_{vdw}\epsilon = \chi_{vdw}k_B T$, and for $\chi_{vdw} = 1$, one recovers the standard attractive component of the LJ-potential [see Eq.

TABLE I: Model simulation parameters with some fixed values.

Parameters	
$T = 298K$	room temperature
$Z_M = 40$	macroion valence
$Z = 1$	microion valence
$\sigma = 4.25 \text{ \AA}$	microion diameter
$l_B = 1.68\sigma = 7.14 \text{ \AA}$	Bjerrum length
$a = 4.5\sigma$	macroion radius
$r_0 = a + \frac{\sigma}{2} = 5\sigma$	macroion-microion distance of closest approach
$R = 60\sigma$	radius of the outer simulation cell
N_+	number of PCs
N_-	number of PAs
$N_{PE} = N_+ + N_-$	total number of polyelectrolyte chains
N_m	number of monomers per chain
χ_{vdw}	strength of the specific van der Waals attraction

(5)]. Since it is not straightforward to link this strength of adsorption directly to experimental values, we therefore investigated different possible strengths of attraction, which are known to be realistic for soft matter systems.

All the simulation parameters are gathered in Table I. The set of simulated systems can be found in Table II. Single-particle moves were considered with an acceptance ratio of 20 – 30% for the monomers and 50% for the counterions. At equilibrium, the (average) length of the trial moves Δr are about 30σ for the counterions and 0.1σ for the monomers. About 10^5 to 10^6 MC steps per particle were required for equilibration, and about 2×10^6 subsequent MC steps were used to perform measurements.

III. TARGET QUANTITIES

Before presenting the results, we briefly describe the different observables that are going to be measured. Of first importance, we compute the radial density of monomers $n_{\pm}(r)$ around the spherical macroion normalized as follows

$$\int_{r_0}^R 4\pi r^2 n_{\pm}(r) dr = N_{\pm} N_m \quad (7)$$

where (+)– applies to PCs (PAs). This quantity is of special interest to characterize the degree of ordering in the vicinity of the macroion surface.

TABLE II: System parameters. The number of counterions (cations and anions) ensuring the overall electroneutrality of the system is not indicated.

System	N_{PE}	N_+	N_-	N_m
<i>A</i>	1	1	0	80
<i>B</i>	2	1	1	80
<i>C</i>	3	2	1	80
<i>D</i>	4	2	2	80
<i>E</i>	5	3	2	80
<i>F</i>	6	3	3	80
<i>G</i>	12	6	6	80
<i>H</i>	40	20	20	10

The total number of accumulated monomers $\bar{N}_{\pm}(r)$ within a distance r from the macroion center is then given by

$$\bar{N}_{\pm}(r) = \int_{r_0}^r 4\pi r'^2 n_{\pm}(r') dr' \quad (8)$$

where (+)– applies to PCs (PAs). This observable will be used for the study of the adsorption of (i) a single PC chain (Sec. IV) and (ii) two oppositely charged polyelectrolytes (Sec. V).

Another quantity of special interest is the global *net fluid charge* $Q(r)$ which is defined as follows

$$Q(r) = \int_{r_0}^r 4\pi r'^2 Z [\tilde{n}_+(r') - \tilde{n}_-(r')] dr', \quad (9)$$

where \tilde{n}_+ (\tilde{n}_-) include the density of all the positive (negative) microions. Thus, $Q(r)$ corresponds to the total fluid charge (omitting the macroion bare charge Z_M) within a distance r from the macroion center, and at the cell wall $Q(r = R) = Z_M$. Up to a factor proportional to $1/r^2$, $[Q(r) - Z_M]$ gives (by simple application of the Gauss theorem) the mean electric field at r . Therefore $Q(r)$ can measure the strength of the macroion charge screening by the charged species present in its surrounding solution.

IV. SINGLE CHAIN ADSORPTION

In this part, we study the adsorption of a single long PC chain (system *A*) for different couplings χ_{vdw} . Experimentally this would correspond to the process of the *first* polyelectrolyte layer formation.

The monomer density $n_+(r)$ and fraction $\bar{N}_+(r)/N_m$ are depicted in Fig. 1(a) and Fig. 1(b), respectively. The density $n_+(r)$ near contact ($r \sim r_0$) increases considerably with χ_{vdw} as expected. At a radial distance of 1.5σ from the macroion surface (i.e., $r = r_0 + \sigma$), more than 97% of the monomers are adsorbed for sufficiently large χ_{vdw} (here $\chi_{vdw} > 3$) against only 78% for $\chi_{vdw} = 0$.

The net fluid charge $Q(r)$ is reported in Fig. 2. In all cases we observe a macroion charge reversal (i.e., $Q(r)/Z_M > 1$), as expected from previous studies [27, 28] addressing only $\chi_{vdw} = 0$. The position $r = r^*$ at which $Q(r^*)$ gets its maximal value decreases with χ_{vdw} , due to the χ_{vdw} -enhanced adsorption of the chain. This *overcharging* increases with χ_{vdw} , since the gain in energy by macroion-monomer VDW interactions can better overcome (the higher χ_{vdw}) the cost of the self-energy stemming from the adsorbed excess charge. Note

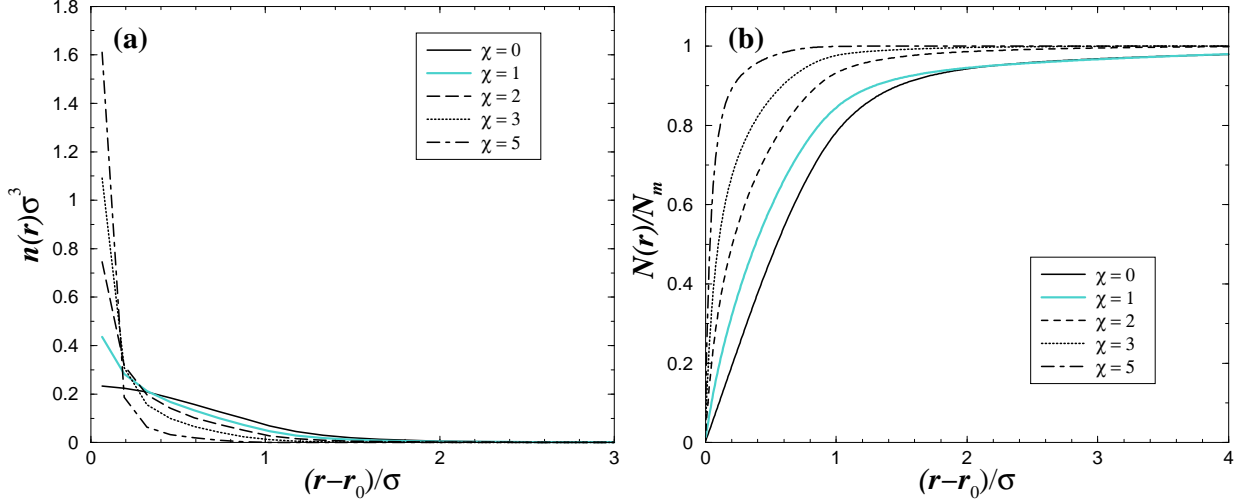


FIG. 1: Monomer adsorption profiles of a single PC-chain (system A) at different χ_{vdw} couplings. (a) radial density $n_+(r)$. (b) fraction of monomers $\bar{N}_+(r)/N_m$.

that the maximal value of charge reversal of 100% allowed by the total PC charge (i.e., $Q(r^*)/Z_M = 2$) can not be reached due to a slight accumulation of microanions.

Typical equilibrium configurations can be found in Fig. 3. For all χ_{vdw} values, there is a wrapping of the chain around the macroion. In parallel, one can clearly see that the formation of chain loops is gradually inhibited by increasing χ_{vdw} .

Although all the obtained results are intuitively easy to understand, they will turn out

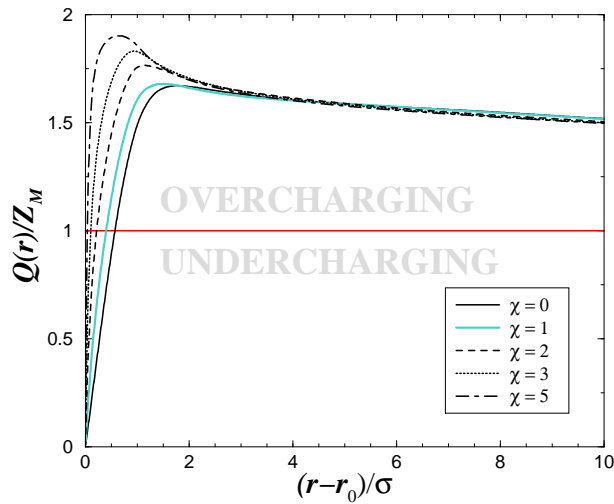


FIG. 2: Net fluid charge $Q(r)$ for system A at different χ_{vdw} couplings. The horizontal line corresponds to the isoelectric point.

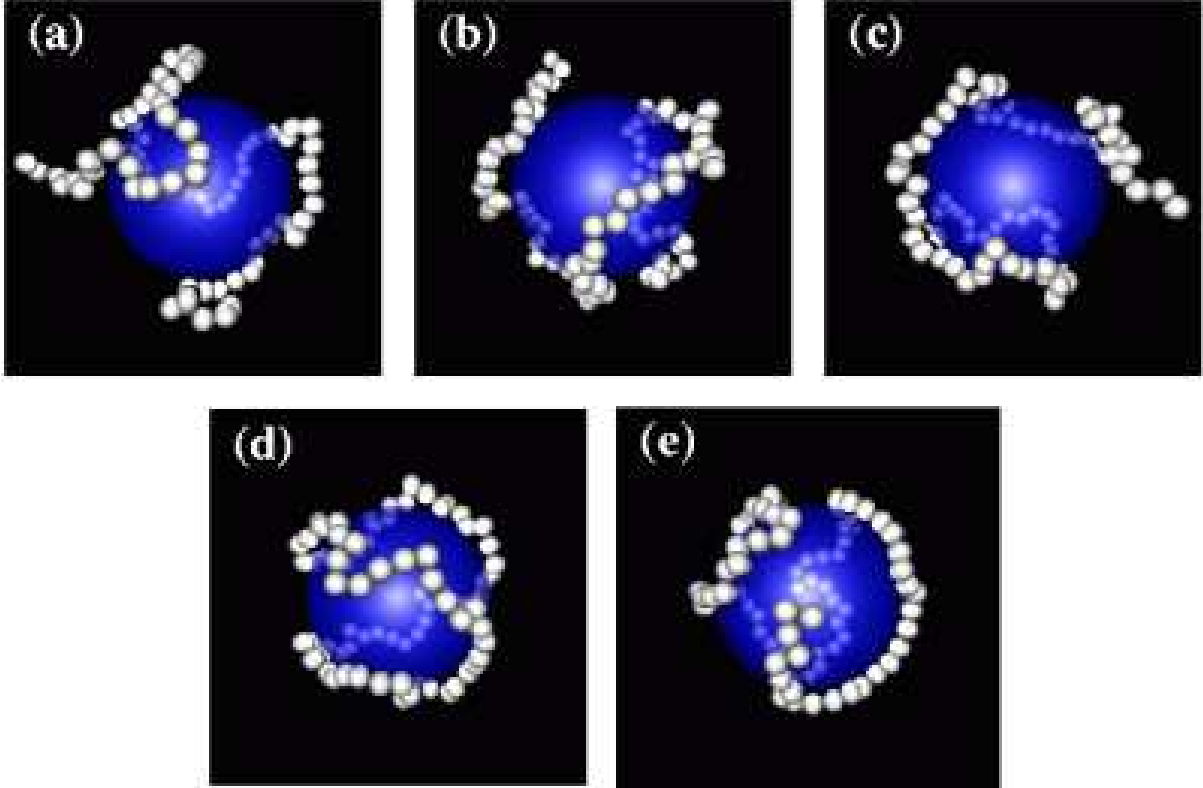


FIG. 3: Typical equilibrium configurations for a single PC adsorbed onto an oppositely charged macroion (system A). The little ions are omitted for clarity. (a) $\chi_{vdw} = 0$ (b) $\chi_{vdw} = 1$ (c) $\chi_{vdw} = 2$ (d) $\chi_{vdw} = 3$ (e) $\chi_{vdw} = 5$.

to be helpful in order to have a quantitative analysis of the effect of an extra short-range attraction already on the level of a single chain adsorption.

V. ADSORPTION OF TWO OPPOSITELY CHARGED POLYELECTROLYTES

We now consider the case where we have additionally a PA chain (system B), so that we have a neutral polyelectrolyte complex (i.e., one PC and one PA). Experimentally this would correspond to the process of the *second* polyelectrolyte layer formation (with system A as the initial state). We stress the fact that this process is fully reversible for the parameters investigated in our present study. In particular, we checked that the same final *equilibrium* configuration is obtained either by (i) starting from system A and then adding a PA or (ii) starting with no chains and then adding the two oppositely charged polyelectrolytes, together with their counterions, simultaneously.

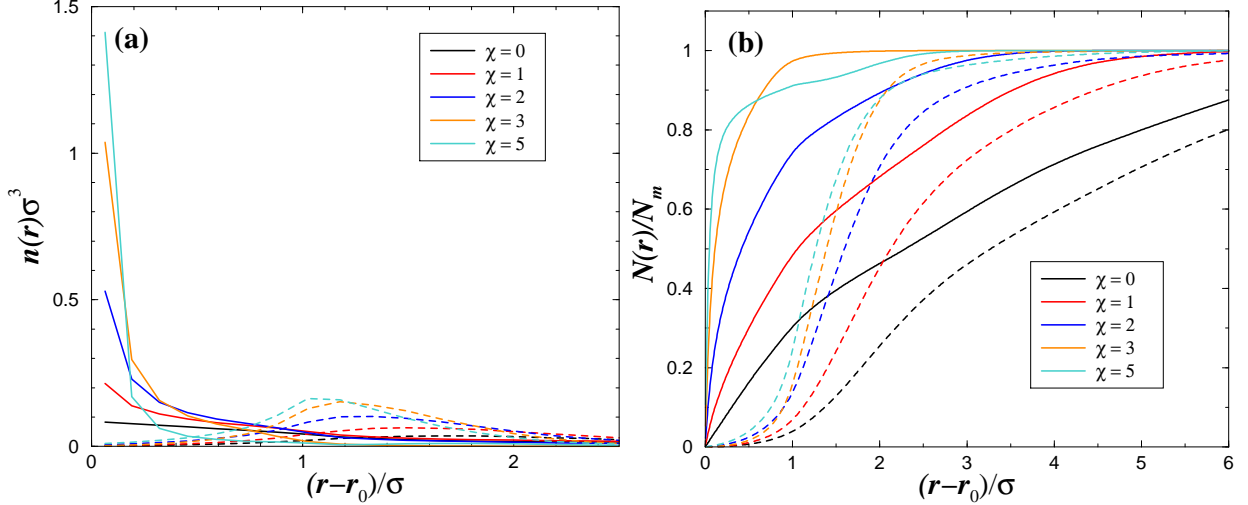


FIG. 4: Monomer adsorption profiles of two polyelectrolyte chains (system B) at different χ_{vdw} couplings. The solid and dashed lines correspond to PC and PA monomers, respectively. (a) radial density $n_{\pm}(r)$. (b) fraction of monomers $\bar{N}_{\pm}(r)/N_m$.

The monomer density $n_{\pm}(r)$ and fraction $\bar{N}_{\pm}(r)/N_m$ are depicted in Fig. 4(a) and Fig. 4(b), respectively. The corresponding microstructures are sketched in Fig. 5. The density of PC monomers $n_+(r)$ near contact ($r \sim r_0$) increases considerably with χ_{vdw} as expected. However, a comparison with system A (see Fig. 1) indicates that the adsorption of PC monomers (at given χ_{vdw}) is weaker when an additional PA is present. This is consistent with the idea that the PC chain tends to build up a globular state by getting complexed to the PA chain. This feature is well illustrated in Fig. 5. More precisely, for sufficiently small $\chi_{vdw} \lesssim 1$, the polyelectrolyte globular state is highly favorable compared to the "flat" bilayer state (see also Fig. 5). Nevertheless, at sufficiently large $\chi_{vdw} \gtrsim 2$, the first layer made up of PC monomers is sufficiently stable to produce a second layer made up of PA monomers. Thereby, the two chains wrap around the macroion. As far as the PA monomer adsorption is concerned, Fig. 4 shows that $n_-(r)$ always increases with χ_{vdw} . For $\chi_{vdw} = 0$, the polyelectrolyte complex is very close to the globular polyelectrolyte *bulk* state (i.e., in the absence of the macroion). This is a non-trivial result, since naively one would expect a "true" multilayering for any χ_{vdw} . It is only for large $\chi_{vdw} \gtrsim 3$ that one gets a true bilayer formation, where there is a pronounced peak in $n_-(r)$ around $r - r_0 \approx \sigma$.

It is useful to introduce the following dimensionless interaction parameters $\Gamma_M = Z_M Z \frac{l_B}{r_0}$, which measures the strength of the macroion-PC electrostatic attraction, and $\Gamma_m = Z^2 \frac{l_B}{\sigma}$

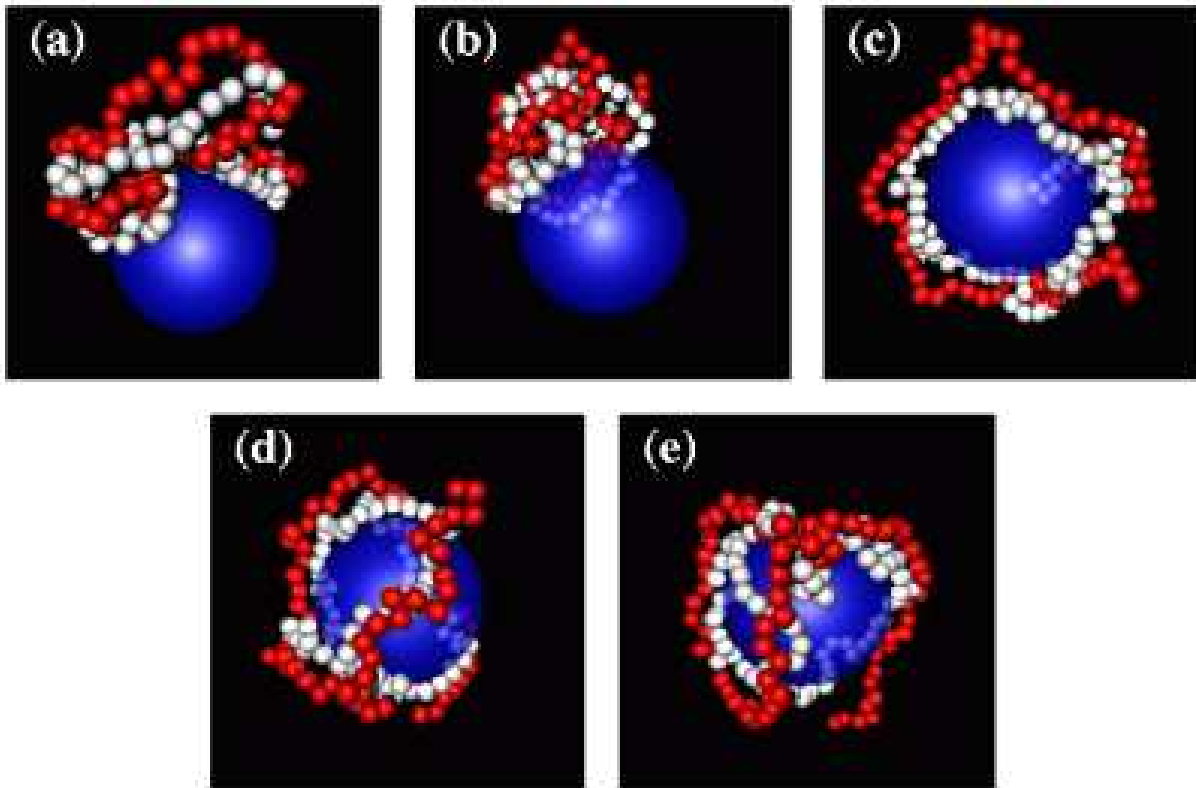


FIG. 5: Typical equilibrium configurations for one PC (in white) and one PA (in red) adsorbed onto the charged macroion (system B). The little ions are omitted for clarity. (a) $\chi_{vdw} = 0$ (b) $\chi_{vdw} = 1$ (c) $\chi_{vdw} = 2$ (d) $\chi_{vdw} = 3$ (e) $\chi_{vdw} = 5$.

which controls the PC-PA complex interaction. For large values of Γ_m the bulk complex will always be in a globular state, since then the Coulomb interaction will give rise to a chain collapse, similar to those seen in polyelectrolyte systems. Thus, for a sufficiently large value of Γ_m/Γ_M at given χ_{vdw} , the globular state will always be favorable and no bilayering can occur. In this case *unwrapping* occurs, similarly to the microstructures depicted in Fig. 5(a) and Fig. 5(b). On the other hand, we find at fixed parameters Γ_m and Γ_M , that one needs a sufficiently large value χ_{vdw}^* , in order to achieve bilayering.

One can summarize these important results as follows:

- The equilibrium *bilayering* process on a spherical charged colloid with long polyelectrolyte chains requires a sufficiently strong extra short-ranged macroion-PC attraction.

A closer look on Fig. 4(b) reveals a further non-trivial behavior in the profiles of $\bar{N}_{\pm}(r)$ at high χ_{vdw} . Very close to the macroion surface we always have a monotonic behavior of

the fraction of adsorbed PC [$\bar{N}_+(r; \chi_{vdw})$] and PA monomers [$\bar{N}_-(r; \chi_{vdw})$] with respect to χ_{vdw} as it should be. However, for a certain distance away from the surface we observe an unexpected behavior where $\bar{N}_+(r; \chi_{vdw} = 3) > \bar{N}_+(r; \chi_{vdw} = 5)$ as well as $\bar{N}_-(r; \chi_{vdw} = 3) > \bar{N}_-(r; \chi_{vdw} = 5)$. One can qualitatively explain this effect by the onset of the formation of one (or several) polyelectrolyte microglobule(s), i.e., small cluster(s) of oppositely charged monomers [see Figs. 5 (d) and (e)]. This is indeed possible because at high χ_{vdw} in principle more PC (and consequently also PA) monomers want to get close to the macroion surface. Already for neutral chains a two dimensional flat adsorbed chain needs a high (surface) binding energy. Compared to bulk conformations the chain entropy is roughly reduced by $k_B T N \ln(q_{d=2}/q_{d=3})$. Here q is the effective number of conformational degrees of freedom of a bond, giving that $\ln(q_{d=2}/q_{d=3}) = O(1)$. Thus local microglobules that induce a small local desorption, are entropically much more favorable. Also, on the level of the energy, an increase of q concomitantly favors the PC-PA microglobule.

The net fluid charge $Q(r)$ is reported in Fig.6. For $\chi_{vdw} \gtrsim 2$ the macroion gets even overcharged and undercharged as one gets away from its surface, whereas for low χ_{vdw} no *local* overcharging occurs. Again, at high χ_{vdw} the strength of the charge oscillation is not a monotonic function of χ_{vdw} where we observe a higher local overcharging (and undercharging) with $\chi_{vdw} = 3$ than with $\chi_{vdw} = 5$. This latter feature is fully consistent with the profiles

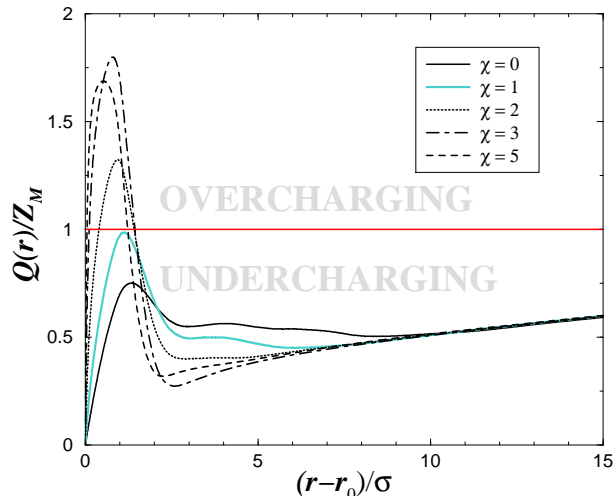


FIG. 6: Net fluid charge $Q(r)$ for system B at different χ_{vdw} couplings. The horizontal line corresponds to the isoelectric point.

of $\bar{N}_{\pm}(r)$ [see Fig. 4(b)] previously discussed [29]. However this onset of local (surface) microglobules (for $\chi_{vdw} = 5$) is not strong enough to produce a non-monotonic behavior of r^* with respect to χ_{vdw} .

VI. MULTILAYERING

We now turn to the case where there are many polyelectrolytes (with $N_{PE} \geq 3$) in the system. We recall that when $\chi_{vdw} \neq 0$, the VDW interaction concern monomers of all PCs lying within the range of interaction. To keep the number of plots manageable, we will present our results obtained for $\chi_{vdw} = 0$ and $\chi_{vdw} = 3$. The case $\chi_{vdw} = 0$ is (conceptually) important since it corresponds to the situation where only purely electrostatic interactions are present. The other case $\chi_{vdw} = 3$ seems to be a reasonable choice, since we found a "true" bilayering for that value. Moreover, such a strength should be easily accessible experimentally.

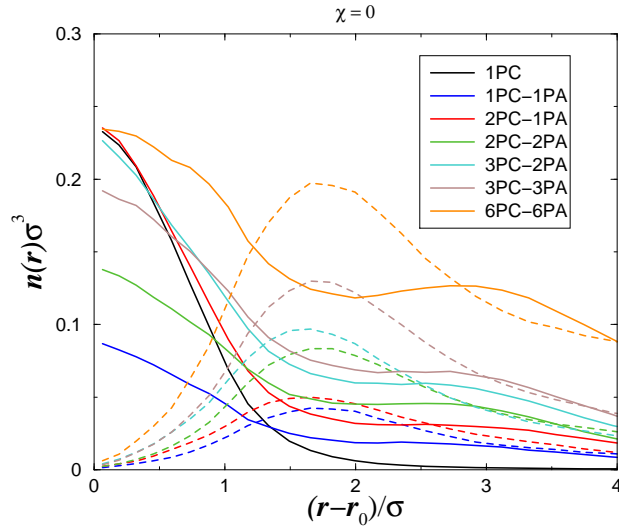


FIG. 7: Radial monomer density for the systems $A - G$ with $\chi_{vdw} = 0$. The solid and dashed lines correspond to $n_+(r)$ and $n_-(r)$, respectively. The number of PC and PA chains is indicated. The plots of $n_{\pm}(r)$ for the systems A (1PC) and B (1PC-1PA) are again reported here for direct comparison.

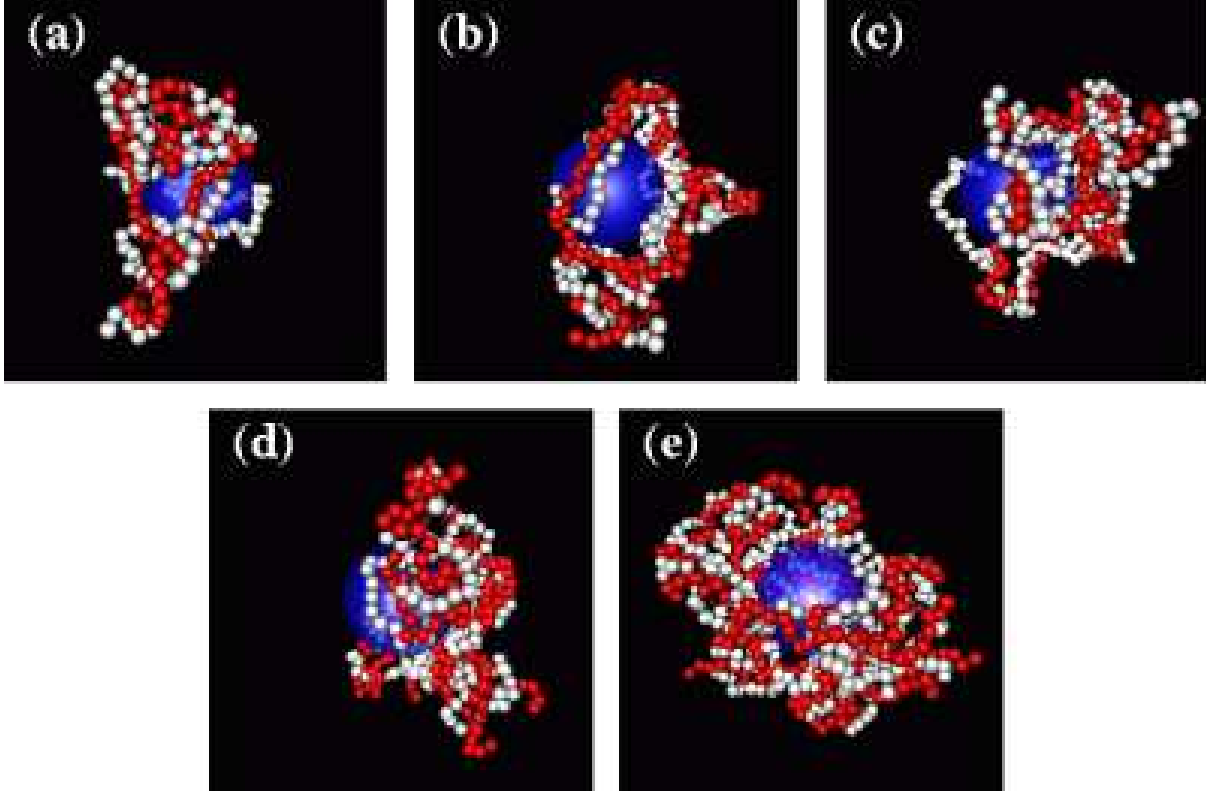


FIG. 8: Typical equilibrium configurations for *many* polyelectrolyte chains adsorbed onto the charged macroion with $\chi_{vdw} = 0$. The PC monomers are in white and PA ones in red. The little ions are omitted for clarity. (a) 2PC-1PA (system *C*) (b) 2PC-2PA (system *D*) (c) 3PC-2PA (system *E*) (d) 3PC-3PA (system *F*) (e) 6PC-6PA (system *G*).

A. Adsorption with $\chi_{vdw} = 0$

The density profiles of $n_{\pm}(r)$ for the systems *A* – *G* (with $\chi_{vdw} = 0$) are reported in Fig. 7 and the corresponding microstructures are sketched in Fig. 8.

Figure 7 shows that when the total polyelectrolyte charge,

$$Q_{PE} \equiv (N_+ - N_-)N_m e, \quad (10)$$

is zero, the density of PC monomers $n_+(r)$ near contact is lower than when charge $Q_{PE} = N_m e$ (recalling that our systems are such that $Q_{PE} = 0$ or $N_m e$). This tendency [lower $n_+(r)$ near contact with $Q_{PE} = 0$] gradually decreases as the total number N_{PE} of polyelectrolytes is increased. In particular for the system *G* where $N_{PE} = 12$ and $Q_{PE} = 0$, the density $n_+(r)$ near contact is nearly identical to that of systems *A*, *C* and *E* where $Q_{PE} = N_m e$.

On the other hand, when $Q_{PE} = N_m e$ then $n_+(r)$ near contact is nearly independent of N_{PE} . The height of the peak in the PA monomer density $n_-(r)$ *increases monotonically* with N_{PE} . Concomitantly, a *third* layer made of PC monomers builds up for high enough N_{PE} . This multilayering is especially remarkable for $N_{PE} = 12$ (system *G*).

All these features concerning the *first* layer structure can be rationalized with simple ideas. When $Q_{PE} = 0$, then the resulting global attraction between the macroion and the polyelectrolyte complex is much weaker than when $Q_{PE} = N_m e$. In this latter situation where $Q_{PE} = N_m e$, this excess charge carried by a PC chain leads to a relatively strong PC adsorption near the surface. The equilibrium configurations sketched in Fig. 8 suggest a wrapping from the PC monomers when $Q_{PE} = N_m e$ [see Fig. 8(a) and (c)] and a (partial) *unwrapping* when $Q_{PE} = 0$ [see Fig. 8(b), (d)]. Even for high $N_{PE} = 12$ [see Fig. 8(e)], we can see this tendency of unwrapping leading to a polyelectrolyte-complex globular state. However, for symmetry reasons, when the total number of monomers is large enough as it is the case with $N_{PE} = 12$, the distribution of the polyelectrolyte complex gets more isotropic leading to a weaker unwrapping at $Q_{PE} = 0$.

The collapse into a globular polyelectrolyte complex becomes even more spectacular when σ is reduced (i.e., larger Γ_m) [30]. In that case (not reported here), we found a wrapping (for $Q_{PE} = N_m e$) similar to that depicted in Fig. 8(a) and (c), and a *strong* unwrapping (for $Q_{PE} = 0$) where the compact neutral polyelectrolyte complex is adsorbed onto a small area of the colloid.

The net fluid charge $Q(r)$ is reported in Fig. 9. As expected one detects an overcharging and undercharging for $Q_{PE} = N_m e$ and $Q_{PE} = 0$, respectively. For $Q_{PE} = 0$, the macroion is also locally overcharged very close to the macroion surface and its strength increases with N_{PE} . On the other hand, the strength of the undercharging (occurring at the largest radial position r^* of the extrema) at $Q_{PE} = 0$ is nearly independent of N_{PE} . In parallel, the strength of the overcharging (occurring at the largest radial position r^* of the extrema) measured at $Q_{PE} = N_m e$ is also nearly independent of N_{PE} (systems *C* and *E*). Moreover, our simulations show that for $N_{PE} \geq 2$ the strength of the overcharging (with $Q_{PE} = N_m e$) and undercharging (with $Q_{PE} = 0$) have nearly the same amplitude, in qualitative agreement with experimental data.

B. Adsorption with $\chi_{vdw} \neq 0$

In this part, we consider the additional attractive VDW macroion-PC monomer interaction with $\chi_{vdw} = 3$. The same investigation as with $\chi_{vdw} = 0$ is carried out here.

The density profiles of $n_{\pm}(r)$ for the systems $A - G$ (with $\chi_{vdw} = 3$) are reported in Fig. 10 and the corresponding microstructures are sketched in Fig. 11.

Figure 10 shows that the density $n_{+}(r)$ near contact (for a given system) is about six times larger than that obtained at $\chi_{vdw} = 0$ (compare Fig. 7). When $Q_{PE} = N_m e$, the density $n_{+}(r)$ at contact (slightly) increases monotonically with N_{PE} in contrast to what happened at $\chi_{vdw} = 0$ where it was nearly independent of N_{PE} . When $Q_{PE} = 0$, we remark that the density $n_{+}(r)$ near contact is nearly independent of N_{PE} (for $N_{PE} \geq 2$) in contrast to what happened at $\chi_{vdw} = 0$.

As far as the PA density $n_{-}(r)$ is concerned, the height of the first peak (for a given system) is about twice larger than that obtained at $\chi_{vdw} = 0$. This height is a monotonic function of N_{PE} *within* a given regime of Q_{PE} (here, either 0 or $N_m e$). Nevertheless, in general this height exhibits a non-trivial dependence on N_{PE} , in contrast to our results with $\chi_{vdw} = 0$. For the systems B and C both containing a single PA chain ($N_- = 1$), the height of the first peak in $n_{-}(r)$ is smaller with $N_+ = 2$ (system C) than with $N_+ = 1$ (system

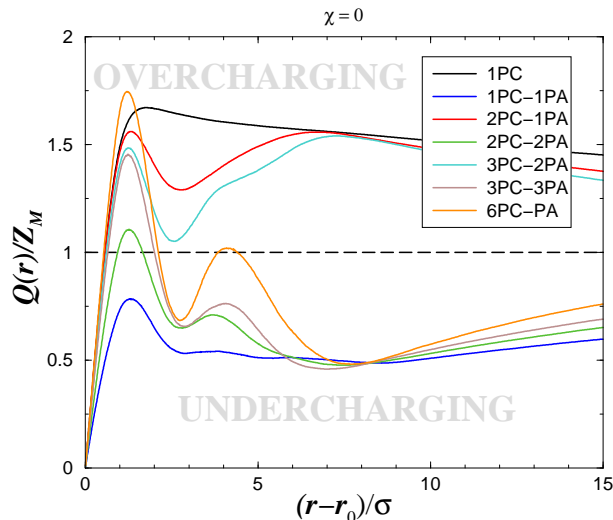


FIG. 9: Net fluid charge $Q(r)$ for the systems $A - G$ with $\chi_{vdw} = 0$. The number of PC and PA chains is indicated. The plots for the systems A (1PC) and B (1PC-1PA) are again reported here for direct comparison. The horizontal line corresponds to the isoelectric point.

B). This is again due to the formation of clusters of oppositely charged monomers that takes place *above* the first layer. This effect is more pronounced when the amount of PC monomers (at given N_-) is larger (system *C*), leading to a local desorption of PA monomer. Those features are remarkable by a comparison of the snapshots of the systems *B* and *C* depicted in Fig. 5(d) and Fig. 11(a), respectively. Similar arguments can be used for the systems *D* and *E*, where the same effect is found. At large N_{PE} , the height of the first peak in $n_-(r)$ saturates as expected.

For $3 \leq N_{PE} \leq 6$, our simulation shows that the formation of the *third* layer [i.e., the second peak in $n_+(r)$ at $r - r_0 \approx 2.6\sigma$] is enhanced when $Q_{PE} = N_m e$ at fixed N_+ . This effect can again be explained in terms of polyelectrolyte (micro)globules formation. Indeed, above the *second* layer, the formation of clusters made up of oppositely charged monomers is enhanced when the polyelectrolyte complex (seen by the underneath bilayer) is uncharged which corresponds to a state of charge $Q_{PE} = 0$.

It is interesting to see that with $N_{PE} = 12$ one even gets a second peak (and not a shoulder) in $n_-(r)$, which is the signature of a *fourth* layer. This qualitatively contrasts with our findings at $\chi_{vdw} = 0$. Therefore, we conclude that the effect of an extra short-ranged macroion-PC attraction is crucial for the multilayering process.

On a more qualitative level, it is very insightful to compare the microstructures obtained with purely electrostatic interactions ($\chi_{vdw} = 0$) sketched in Fig. 8 with those obtained

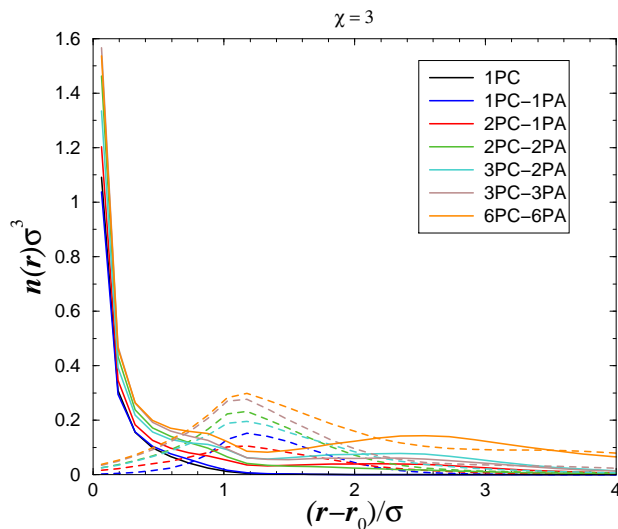


FIG. 10: Same as Fig. 7 but with $\chi_{vdw} = 3$.

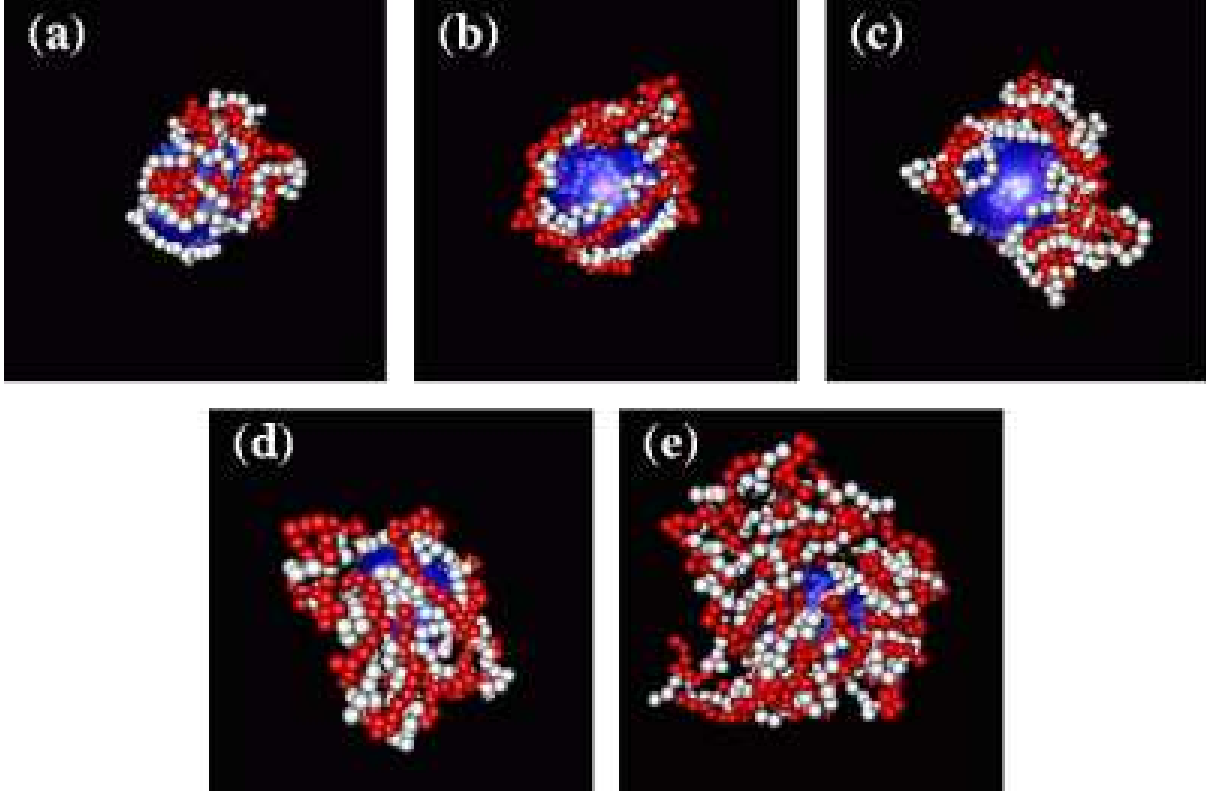


FIG. 11: Same as Fig. 8 but with $\chi_{vdw} = 3$. (a) 2PC-1PA (system *C*) (b) 2PC-2PA (system *D*) (c) 3PC-2PA (system *E*) (d) 3PC-3PA (system *F*) (e) 6PC-6PA (system *G*).

with a short-ranged VDW macroion-PC interaction ($\chi_{vdw} = 3$) sketched in Fig. 11. From such a visual inspection, it is clear that in all cases the adsorbed polyelectrolyte complex is flatter at $\chi_{vdw} = 3$ than at $\chi_{vdw} = 0$. An other important qualitative difference, is that the *unwrapping* occurring at $\chi_{vdw} = 0$ with $Q_{PE} = 0$ [see Fig. 8(b) and (d)] is no longer effective when $\chi_{vdw} = 3$ [see Fig. 11(b) and (d)]. In the same spirit, for a large number of chains ($N_{PE} = 12$), the macroion surface is only partially covered by the PC monomers where some (large) holes appear [see Fig. 8(e)], in contrast to what occurs at $\chi_{vdw} = 3$, where all the macroion surface is covered [see Fig. 11(e)].

The net fluid charge $Q(r)$ is reported in Fig. 12. As expected one finds an overcharging and undercharging for $Q_{PE} = N_m e$ and $Q_{PE} = 0$, respectively. Now one can get a local overcharging larger than 100% (i.e., $Q(r)/Z_M > 2$) due to the VDW attraction that can lead to a first layer with *many* PC chains. For systems *C* and *E* we see that the overcharging at the third layer is around 50% and nearly independent of N_{PE} .

On the other hand, the strength of the undercharging (occurring at the largest radial

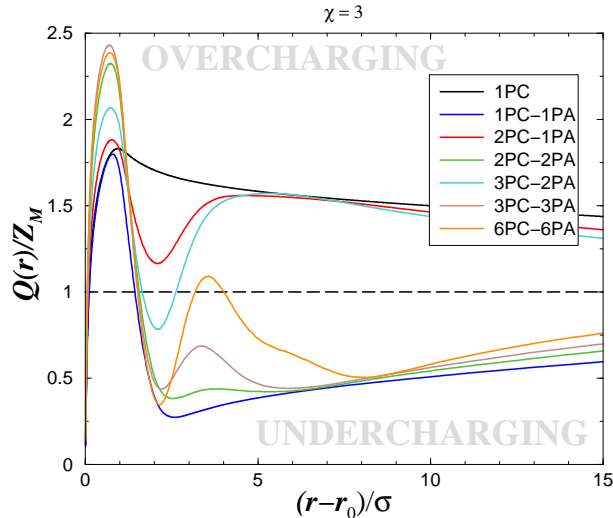


FIG. 12: Same as Fig. 9 but with $\chi_{vdw} = 3$.

position r^* of the extrema) at $Q_{PE} = 0$ decreases with increasing N_{PE} , providing a gradually weaker driving force for the subsequent adsorption of the PC chain. On the basis of our results with $\chi_{vdw} = 0$, we expect that the strength of the undercharging at $\chi_{vdw} = 3$ (for larger N_{PE}) should stabilize around 50%. So it appears that the oscillation of under- and overcharging are not 100%, but rather close to 50%. This is probably sensitive to the specific model parameters chosen. What can be stated from our data is, that there is no reason to find a generally applicable overcharging fraction. Especially for the case of relatively small colloids, the results will strongly depend on the specific system parameters, which are both of electrostatic as well as non-electrostatic nature.

VII. CASE OF SHORT CHAINS

We now investigate the effect of chain length dependence. In this case the adsorption of a single chain does not necessarily produce an overcharging since the chain length ($N_m = 10$ - system H) is too short. The density profiles of $n_{\pm}(r)$ are reported in Fig. 13 for various χ_{vdw} , and the corresponding microstructures are sketched in Fig. 14. In the purely electrostatic regime ($\chi_{vdw} = 0$), the polyelectrolyte adsorption is weak and it significantly increases with χ_{vdw} . However, for all reported cases, we only observe a bilayering in contrast with previous long chain systems (compare Fig. 13 with Fig. 7 and Fig. 10) where thereby a true

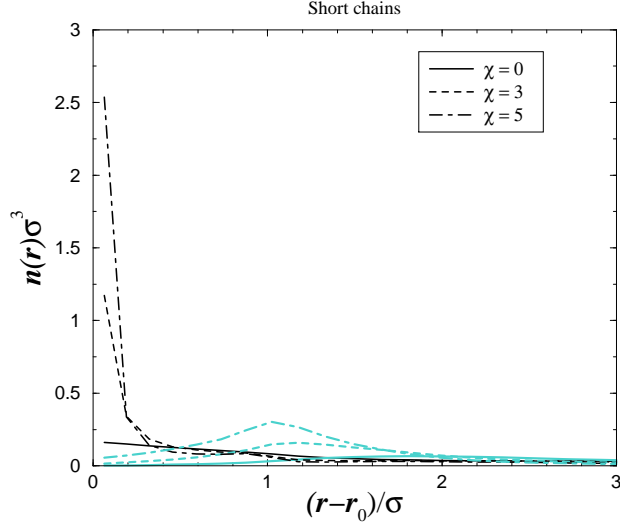


FIG. 13: Radial monomer density for short polyelectrolyte chains (system H) at different χ_{vdw} couplings. The black and gray lines correspond to PC and PA monomers, respectively.

multilayering was reported.

In addition we observe several globally neutral polyelectrolyte complexes in the bulk, whose number decreases with χ_{vdw} (see Fig. 14). This feature was inhibited for long chains due to the strong PC-PA binding energy that keeps all the chains near the macroion surface. At sufficiently strong χ_{vdw} [see Fig. 14(c) with $\chi_{vdw} = 5$], the macroion area gets largely (and *uniformly*) covered by the PC chains, leading to a strong bilayering. Nevertheless, due

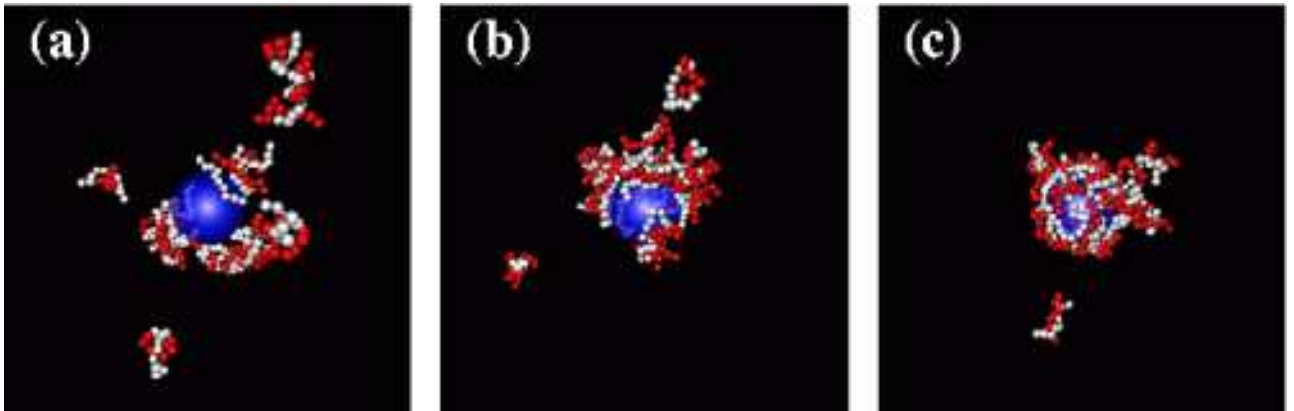


FIG. 14: Typical equilibrium configurations for short PC (in white) and PA (in red) chains adsorbed onto the charged macroion (system H). The little ions are omitted for clarity. (a) $\chi_{vdw} = 0$ (b) $\chi_{vdw} = 3$ (c) $\chi_{vdw} = 5$

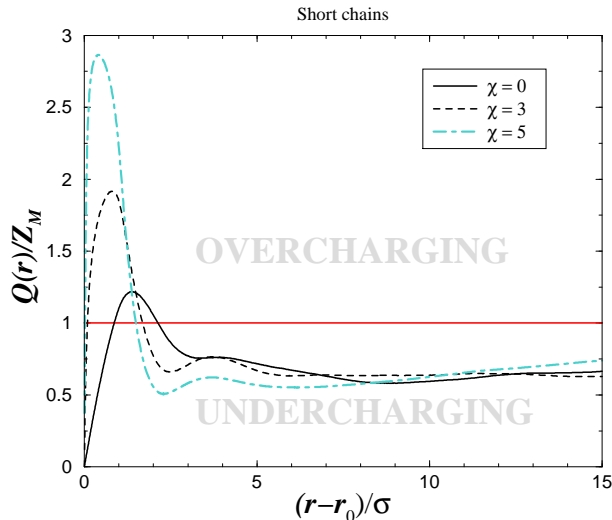


FIG. 15: Net fluid charge $Q(r)$ for system H at different χ_{vdw} couplings. The horizontal line corresponds to the isoelectric point.

to the weak PC-PA binding energy, the formation of additional layer seems to be prohibited in contrast to what was observed at $\chi_{vdw} = 3$ with systems D and E that contain a similar number of monomers. Those observations lead us to the relevant conclusion that multilayering with short chains (if experimentally observed on a charged colloidal sphere) must involve additional non-trivial driving forces like specific PC monomer-PA monomer interactions that are not captured by our model. This again seems to be in agreement with the arguments presented in Ref.[7] which argue against a stable thermodynamic equilibrium complex when there is excess polyelectrolytes present.

The net fluid charge plotted in Fig. 15 indicates that only one charge oscillation (around the isoelectric point) is obtained in contrast to what can happen with longer chains. Again, here the driving force for the bilayer formation is the overcharging that increases with χ_{vdw} .

VIII. CONCLUDING REMARKS

We have carried out MC simulations to study the basic mechanisms involved in forming equilibrium polyelectrolyte complexes on a charged colloidal sphere. This work emphasizes the role of the short-range Van der Waals-like attraction (characterized here by χ_{vdw}) between the spherical macroion surface and the oppositely charged adsorbed chain(s).

It was demonstrated that, for the bilayering process involving two long oppositely charged

chains at fixed Γ_m and Γ_M , it is necessary to have a sufficiently high χ_{vdw} . In particular, below a certain value of $\chi_{vdw} = \chi_{vdw}^*$, a dense adsorbed polyelectrolyte globule is obtained, whereas above χ_{vdw}^* a flat bilayer builds up.

The same qualitatively applies to the case of many (more than two) long polyelectrolytes. In a purely electrostatic regime (i.e., $\chi_{vdw} = 0$) one can never obtain a true (uniform) multilayering. However, by increasing χ_{vdw} , one gradually increases the polyelectrolyte (polycation and polyanion) chain adsorption ultimately leading to a true multilayering where the macroion is uniformly covered. Nonetheless, at given χ_{vdw} and especially for small χ_{vdw} , the polyelectrolyte globular state is always favored when its net charge is zero.

As far as the short chain case is concerned, it was shown that even bilayering can not be reached within the pure electrostatic regime. Only at higher χ_{vdw} (higher than those coming into play with long chains), one recovers a bilayer formation. However, multilayering (beyond bilayering) with very short chains seems to be very unlikely within our model. The large complex would not be thermodynamically stable and dissolve into smaller charge neutral polyelectrolyte complexes, consistent with the ideas presented in Ref.[7].

As an overall conclusion, our results clearly demonstrated that besides an overcharging driving force [i.e., successive macroion (effective) charge reversal by successive polymer layering), the stability of the polyelectrolyte multilayer is strongly influenced by the specific macroion-polyelectrolyte short range attraction. This statement should at least hold for the investigated cases of equilibrium structures.

A future study should systematically study other important effects, such as chain flexibility, specific interchain monomer-monomer interaction, microions valency etc... Nevertheless, our present findings hopefully will generate some further systematic studies to explore the effects of non-electrostatic effects for the layer-by-layer deposition technique.

Acknowledgments

R. M. thanks F. Caruso and S. K. Mayya for helpful and stimulating discussions. This work was supported by *Laboratoires Européens Associés* (LEA) and the SFB 625.

[1] Schmitt, J.; Decher, G.; Hong, G. *Thin Solid Films* **1992**, 210/211, 831.

- [2] Decher, G. *Science* **1997**, *277*, 1232–1237.
- [3] Caruso, F.; Furlong, D. N.; Ariga, K.; Ichinose, I.; Kunitake, T. *Langmuir* **1997**, *14*, 4559–4565.
- [4] Onda, M.; Ariga, K.; Kunitake, T. *Biosci. Bioeng.* **1999**, *87*, 69–75.
- [5] Wu, A.; Yoo, D.; Lee, J. K.; Rubner, M. F. *J. Am. Chem. Soc.* **1999**, *121*, 4883–4891.
- [6] Dijt, J. C.; Cohen-Stuart, M. A.; Fleer, G. J. *J. Adv. Colloid Interface Sci.* **1994**, *50*, 79–101.
- [7] Kovacevic, D.; van der Burgh, S.; Cohen-Stuart, M. A. *Langmuir* **2002**, *18*, 5607–5612.
- [8] Schmitt, J.; Grünewald, T.; Decher, G.; Pershan, P.S.; Kjaer, K.; Lösche, M. *Macromol.* **1993**, *26*, 7058–7063.
- [9] Lösche, M.; Schmitt, J.; Decher, G.; Bouwman, W. G.; Kjaer, K. *Macromolecules* **1998**, *31*, 8893–8906.
- [10] McAloney, R. A.; Sinyor, M.; Dudnik, V.; Goh, M. C. *Langmuir* **2001**, *17*, 6655–6663.
- [11] Schoeler, B.; Kumaraswamy, G.; Caruso, F. *Macromolecules* **2002**, *35*, 889–897.
- [12] McCormick, M., Smith, R., Graf, R., Barrett C.J., Reven L., Spiess, H.W., preprint
- [13] Lowack, K.; Helm, C. A. *Macromolecules* **1998**, *31*, 823–833.
- [14] Caruso, F.; Carsuo, R. A.; Möhlwald, H. *Science* **1998**, *282*, 1111–1114.
- [15] Gittins, D. I.; Caruso, F. *J. Phys. Chem. B* **2001**, *105*, 6846–6852.
- [16] Netz, R. R.; Joanny, J. F. *Macromolecules* **1999**, *32*, 9013–9025.
- [17] Castelnovo, M.; Joanny, J. F. *Langmuir* **2000**, *16*, 7524–7532.
- [18] Farhat, T.; Yassin, G.; Dubas, S. T.; Schlenoff, J. B. *Langmuir* **1999**, *15*, 6621–6623.
- [19] Joanny, J. F. *Eur. Phys. J. B* **1999**, *9*, 117–122.
- [20] Messina, R.; Holm, C.; Kremer, K. *Phys. Rev. E* **2002**, *65*, 041805.
- [21] Messina, R.; Holm, C.; Kremer, K. *J. Chem. Phys.* **2002**, *117*, 2947–2960.
- [22] Messina, R. *J. Chem. Phys.* **2002**, *117*, 11062–11074.
- [23] Metropolis, N.; Rosenbluth, A. W.; Rosenbluth, M. N.; Teller, A. N.; Teller, E. *J. Chem. Phys.* **1953**, *21*, 1087.
- [24] Allen, M. P.; Tildesley, D. J. *Computer Simulations of Liquids*; Clarendon Press: Oxford, 1987.
- [25] Only the monomer-monomer excluded volume interaction was not modelled by a hard-sphere potential. There, a purely repulsive Lennard-Jones potential was used.
- [26] Kremer, K. *Computer Simulation in Chemical Physics*; Kluwer Academic Publishers: Ams-

terdam, 1993.

[27] Wallin, T.; Linse, P. *Langmuir* **1996**, *12*, 305–314.

[28] Wallin, T.; Linse, P. *J. Phys. Chem.* **1996**, *100*, 17873–17880.

[29] Here we assume the presence of little counterions to be negligible in the vicinity of the macroion surface, which is a very good approximation.

[30] Messina, R. unpublished data.